

# APPLICATION OF MACHINE LEARNING TO PREDICT THE RESPONSE OF THE LIQUID MERCURY TARGET AT THE SPALLATION NEUTRON SOURCE\*

L. Lin<sup>†</sup>, H. Tran, S. Gorti, J. Mach, D. Winder  
Oak Ridge National Laboratory, Oak Ridge, TN, USA

## Abstract

The Spallation Neutron Source (SNS) at Oak Ridge National Laboratory is currently the most powerful accelerator-driven neutron source in the world. The intense proton pulses strike on SNS's mercury target to provide bright neutron beams, which also leads to severe fluid-structure interactions inside the target. Prediction of resultant loading on the target is difficult particularly when helium gas is intentionally injected into mercury to reduce the loading and mitigate the pitting damage on the target's internal walls [1, 2]. Leveraging the power of machine learning and the measured target strain, we have developed machine learning surrogates [3] for modelling the discrepancy between simulations and experimental strain data. We then employ these surrogates to guide the refinement of the high-fidelity mercury/helium mixture model to predict a better match of target strain response.

## MANUSCRIPTS

The availability of the first target station (FTS) at the spallation neutron source (SNS) centre is mission-critical to providing a world-class neutron science program at ORNL. However, premature failure of target modules has led to several interruptions to the SNS user program, highlighting the need for robust target design. This project will leverage measured strain data for the target and ML to develop a two-phase constitutive model for mercury/helium in extreme environments to predict and extend the lifetime of future target designs.

## Target Model and Strain Sensors

A typical mercury target running at FTS includes the solid stainless-steel vessel, and the flowing mercury which are illustrated in Fig. 1.

To reveal the internal structure and the mercury flow, Fig. 1 is shown in cut view. The blue and red lines stand for flowing mercury from vessel's inlets to outlet, indicating a lower temperature of mercury (blue) at the beginning and being heated up by the high energy proton pulses at the front nose part (red). The flowing mercury takes away most of the heat generated by the proton, cooled down outside of the vessel to return into the flow loop. Pipes for the injection of helium gas are shown in green lines in Fig. 1, which will help reduce the pressure and pitting damage on the steel vessel [1, 2]. On the external surface of the steel vessel, several strain gages (Fig. 2) are attached to collect the response due to the neutron pulses. Measurements from

these strain sensors help monitor the running status of target, providing important experimental data for target's modelling and simulations as well.

## Target Vessel Cut View

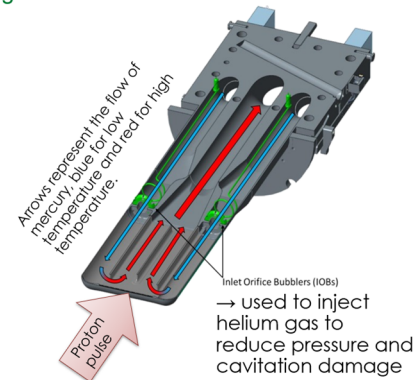


Figure 1: Cut view of mercury Target.

## Strain Sensors on Target Vessel

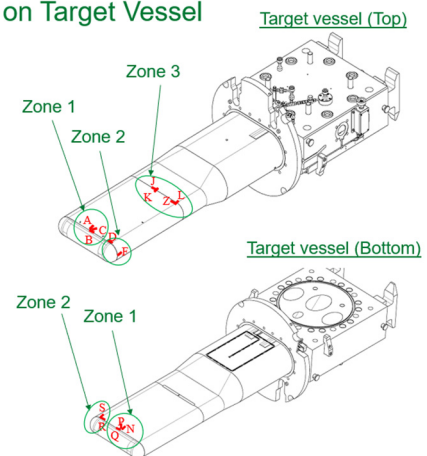


Figure 2: Strain sensors attached on Target's external surface.

## Target Finite Element Simulation

A half symmetric finite element model, as shown in Fig. 3, has been created to simulate the dynamic response of mercury Target due to the proton pulse loads. The proton energy of each pulse deposits on both the mercury and steel parts, being converted into the initial pressure that drives the propagation of stress waves internally. Figure 4 illustrates the contours of this initial pressure field on steel and mercury parts. Obviously, the nose part in the front of target experiences the most extensive initial proton pulse pressure than other locations.

\* Work supported by the Neutron Sciences Directorate at ORNL, and DOE Office of Basic Energy Sciences.

<sup>†</sup> linl@ornl.gov

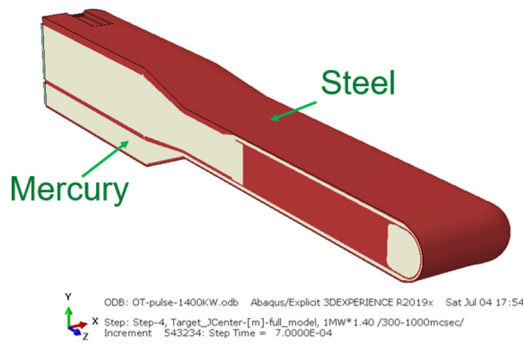


Figure 3: Half symmetric mercury Target model.

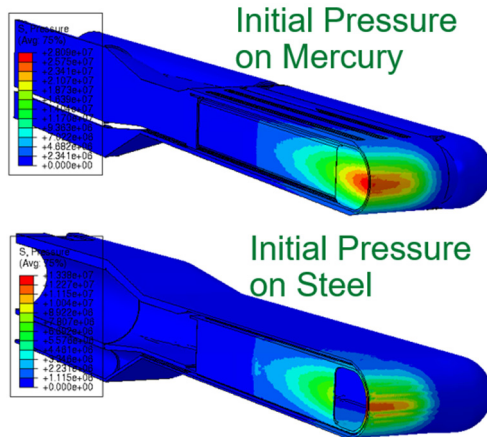


Figure 4: Initial pressure on mercury and steel vessel.

In the Target’s finite element model, an equation of state (EOS) material model is adopted for mercury, with a tensile cut-off value included to represent its cavitation behaviour [4]. Figure 5 demonstrates the stress response at the specific moment after the proton pulse initiates. The red dots in Fig. 5 are selected elements correspond to strain sensors in Fig. 2.

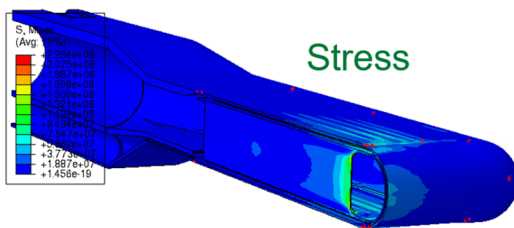


Figure 5: Demonstration of stress response on vessel.

### Tuning Parameters in Mercury Material Model

As mentioned before, helium gas is intentionally injected in the mercury flow in SNS mercury Targets, to mitigate the pitting damage and reduce the vessel pressure therefore to extend target’s lifetime. However, this injected helium bubbles lead to more mismatch between measured target vessel strain and simulation results by using the traditional constitutive mercury model introduced in reference [4]. Figure 6 illustrates this strain discrepancy by comparing the model’s sensor strain history (red curve) and

real strain measurement from sensor (blue curve) at the same location. The strain discrepancy also indicates an improvement on the mercury material model to include the complex bubbles’ behaviour is needed.

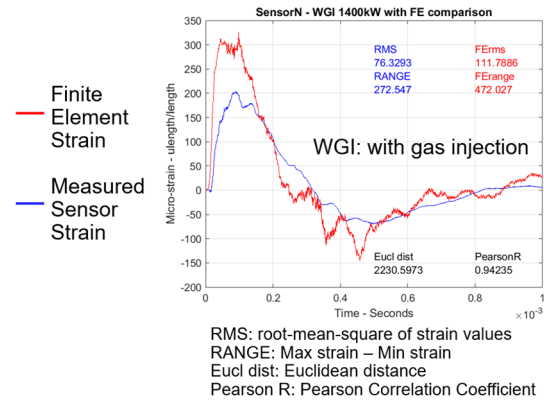


Figure 6: Strain comparison between model and measurement.

Table 1: Tuning Parameters in Mercury Material Model

| Run# | Cut-off (Pa) | Density (kg/m <sup>3</sup> ) | Sound Speed (m/s) |
|------|--------------|------------------------------|-------------------|
| 1    | 1.5517E+06   | 4.3069E+03                   | 4.8793E+03        |
| 2    | 3.1035E+06   | 1.3500E+03                   | 7.9517E+03        |
| 3    | 6.2069E+06   | 2.1948E+03                   | 2.4897E+03        |
| 4    | 1.3966E+07   | 1.0643E+04                   | 3.8552E+03        |
| 5    | 9.8276E+06   | 7.2638E+03                   | 4.5379E+03        |
| 6    | 2.5862E+06   | 5.9966E+03                   | 8.6345E+03        |
| 7    | 1.0000E+01   | 9.7983E+03                   | 7.2690E+03        |
| 8    | 1.0345E+06   | 3.4621E+03                   | 1.1241E+03        |
| 9    | 1.1379E+07   | 1.3178E+04                   | 1.4655E+03        |
| 10   | 1.2414E+07   | 2.6172E+03                   | 2.8310E+03        |
| 11   | 1.1897E+07   | 1.7724E+03                   | 6.5862E+03        |
| 12   | 5.6897E+06   | 1.2333E+04                   | 6.9276E+03        |
| 13   | 4.6552E+06   | 8.1086E+03                   | 5.5621E+03        |
| 14   | 1.3448E+07   | 6.8414E+03                   | 1.8069E+03        |
| 15   | 7.7586E+06   | 3.0397E+03                   | 9.6586E+03        |
| 16   | 7.2414E+06   | 1.1488E+04                   | 3.5138E+03        |
| 17   | 4.1379E+06   | 1.0221E+04                   | 1.0000E+04        |
| 18   | 8.2759E+06   | 7.6862E+03                   | 8.2931E+03        |
| 19   | 1.0345E+07   | 1.1910E+04                   | 9.3172E+03        |
| 20   | 1.5000E+07   | 5.5741E+03                   | 5.2207E+03        |
| 21   | 1.4483E+07   | 8.9534E+03                   | 7.6103E+03        |
| 22   | 6.7241E+06   | 3.8845E+03                   | 6.2448E+03        |
| 23   | 8.7931E+06   | 9.3759E+03                   | 4.4138E+02        |
| 24   | 1.0862E+07   | 1.3600E+04                   | 5.9034E+03        |
| 25   | 3.6207E+06   | 1.1066E+04                   | 7.8276E+02        |
| 26   | 5.1724E+06   | 6.4190E+03                   | 2.1483E+03        |
| 27   | 5.1725E+05   | 8.5310E+03                   | 3.1724E+03        |
| 28   | 2.0690E+06   | 1.2755E+04                   | 4.1966E+03        |
| 29   | 1.2931E+07   | 5.1517E+03                   | 8.9759E+03        |
| 30   | 9.3103E+06   | 4.7293E+03                   | 1.0000E+02        |
| 31   | 1.5000E+07   | 5.3310E+03                   | 1.0000E+03        |
| 32   | 1.5000E+07   | 5.6370E+03                   | 1.5000E+03        |
| 33   | 0.0000E+00   | 1.1762E+04                   | 2.2500E+03        |
| 34   | 1.5000E+07   | 5.3310E+03                   | 7.5000E+02        |

Content from this work may be used under the terms of the CC BY 3.0 licence (© 2021). Any distribution of this work must maintain attribution to the author(s), title of the work, publisher, and DOI

Due to the difficulties of observing the actual mercury behaviour inside the steel vessel under the high proton pulses and radiation environment, more efforts in this project are focused on finding a constitutive mercury material model to substitute current EOS model that can predict a better match with the experimental strain measurements on steel vessel's external surface. By tuning material parameters as shown in Table 1, the EOS-based constitutive model is utilized as the first trial to improve the model itself. The injected helium gas bubbles change the mercury-gas mixture's average density, altering the stress wave speed propagated in the liquid-gas medium, therefore leading to unclear behaviour changes that deviate from the current EOS model. To reflect these changes in mercury material model, the parameters of density, stress wave speed and the tensile cut-off threshold are designed as tuneable variables in the standard EOS equations. Varying tensile cut-off, density and sound speed values are randomly selected from Latin hypercube sampling points [5]. Machine learning methods will train on strain data collected from these simulation runs, to find the optimized model parameters inversely that can produce best match with experimental strain data.

### Current Machine Learning Result

By comparing with one set of experimental strain sensor data, 34 sets of FE sensor data extracted from the simulations listed in Table 1 build trial ML surrogates. Projections of trial surrogate parameters (Fig. 7) on random 2d planes show multimodality, which indicates some optimized parameters that can reduce the strain discrepancy in FE simulation due to the existence of gas bubbles.

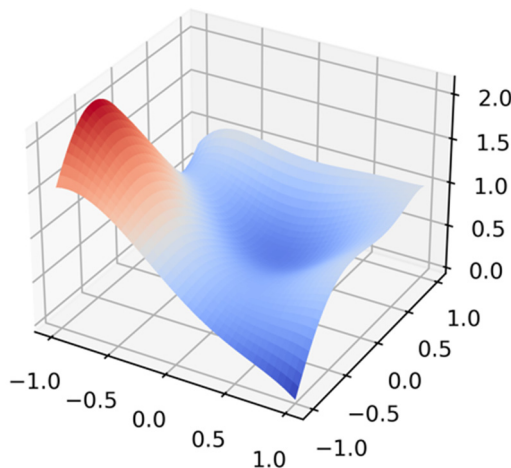


Figure 7: Projections of surrogates on random 2d planes.

The Iso-surface plot of these surrogate parameters (Fig. 8) also shows regions that likely contain candidate parameters for this inverse optimization problem. The identified regions in Fig. 8 will also help refine the parameters search space in next stage.

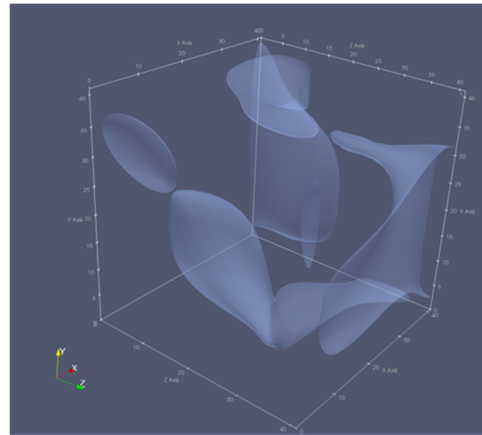


Figure 8: Iso-surface plot of the ML surrogates for the three parameters.

## CONCLUSION

Initial effort in this project introduces varying parameters into traditional EOS-based mercury material model, seeking an improved constitutive model to include bubbles' behaviour into mercury material. Work reported in this poster also builds the preliminary framework to integrate parametric finite element simulation with machine learning for solving the inverse problem. Due to the limited number of finite element simulations, current results only show the candidate regions that likely have the optimized parameters set. Future work includes 1) introduce more physics-based bubble models into mercury material model for parameter tuning; 2) increase the number of FE simulations to improve the accuracy of machine learning surrogates and enable more machine learning methods; and 3) refine the parameter space and develop optimization framework for an efficient parameter search.

## ACKNOWLEDGEMENTS

The authors are grateful for support from the Neutron Sciences Directorate at ORNL in the investigation of this work. This work was supported by the DOE Office of Science (Office of Basic Energy Sciences, Scientific User Facilities program).

Notice: This manuscript has been authored by UT-Battelle, LLC, under contract DE-AC05-00OR22725 with the US Department of Energy (DOE). The US government retains and the publisher, by accepting the article for publication, acknowledges that the US government retains a nonexclusive, paid-up, irrevocable, worldwide license to publish or reproduce the published form of this manuscript, or allow others to do so, for US government purposes. DOE will provide public access to these results of federally sponsored research in accordance with the DOE Public Access Plan (<http://energy.gov/downloads/doe-public-access-plan>).

## REFERENCES

- [1] Y. Liu *et al.*, “Strain measurement in the recent SNS mercury target with gas injection”, *Journal of Physics: Conference Series*, vol. 1067, p. 052022, 2018.  
doi:10.1088/1742-6596/1067/5/052022
- [2] K. Okita *et al.*, “Multi-scale analysis on cavitation damage and its mitigation for the spallation neutron source”, in *Proc. of the 4th International Conference on Computational Methods for Coupled Problems in Science and Engineering (COUPLED PROBLEMS 2011)*, Kos, Greece, Jun. 2011, pp. 600-610.
- [3] A. Chkifa, N. Dexter, H. Tran, and C. Webster, “Polynomial approximation via compressed sensing of high-dimensional functions on lower sets”, *Mathematics of Computation*, vol. 87, pp. 1415-1450, 2017. doi:10.1090/mcom/3272
- [4] B. W. Riemer, “Benchmarking Dynamic Strain Predictions of Pulsed Mercury Spallation Target Vessels”, *Journal of Nuclear Materials*, vol. 343, pp. 81-91, 2005.  
doi:10.1016/j.jnucmat.2005.01.026
- [5] *Isight User's Guide*. SIMULIA Execution Engine, Providence, RI, USA, 2017.